Journal of Semiconductors
(2023) 44, 091605
doi: 10.1088/1674-4926/44/9/091605

REVIEWS

A landscape of β-Ga_2O_3 Schottky power diodes

Man Hoi Wong†

Department of Electronic and Computer Engineering, Hong Kong University of Science and Technology, Clear Water Bay, Kowloon, Hong Kong, China

---

Abstract: β-Ga_2O_3 Schottky barrier diodes have undergone rapid progress in research and development for power electronic applications. This paper reviews state-of-the-art β-Ga_2O_3 rectifier technologies, including advanced diode architectures that have enabled lower reverse leakage current via the reduced-surface-field effect. Characteristic device properties including on-resistance, breakdown voltage, rectification ratio, dynamic switching, and nonideal effects are summarized for the different devices. Notable results on the high-temperature resilience of β-Ga_2O_3 Schottky diodes, together with the enabling thermal packaging solutions, are also presented.

Key words: β-Ga_2O_3; Schottky diodes; power device; edge termination; nickel oxide

Citation: M H Wong, A landscape of β-Ga_2O_3 Schottky power diodes[J]. *J. Semicond.*, 2023, 44(9), 091605. https://doi.org/10.1088/1674-4926/44/9/091605

---

1. Introduction

Power electronics represent an ever-changing domain of vibrant research that covers a wide spectrum of materials, physics, devices, and applications concerning power conversion and management[1]. Of relevance to optoelectronic and display technologies are boost converters used to drive display backlights in modern portable electronic devices. Visible-light communication systems have been proposed to make use of high-brightness light-emitting diodes not only for lighting but also for transmitting information by rapidly modulating the intensity of the emitted light using fast drivers based on switched-mode converters. As the critical electric field (E_{cr}) of semiconductors increases super-linearly with increasing bandgap energy[2], ultrawide-bandgap (UWBG) semiconductors can tolerate high fields to enable high-power electronic devices. Apart from applications in power management, UWBG materials emit deep ultraviolet (UV) light and are therefore attractive for extending the working wavelengths of photonic devices beyond the UV–visible (UV–vis) spectrum to enable potential applications in deep-UV optoelectronics, quantum information science, and bio-chemical sensing.

The UWBG binary oxide, β-Ga_2O_3, has attracted significant attention because of its large 4.8-eV bandgap, controllable n-type doping with Si/Sn/Ge, and relatively high electron mobility of ~200 $cm^2/(V{\cdot}s)$[3–6]. With an E_{cr} approximately three times that of SiC and GaN, β-Ga_2O_3 offers greater intrinsic power conversion efficiencies and further expansion of the operating-voltage–switching-frequency power electronics application space. Melt-grown native substrates are available for β-Ga_2O_3, indicating a path to commercially viable β-Ga_2O_3 devices[7, 8]. Due to its wide bandgap, broadband transparency, low cost, and high thermal/chemical stability, β-Ga_2O_3 has also emerged as a new platform for UV–vis nonlinear optics and integrated photonics such as waveguides and solar-blind photodetectors[9, 10].

As an integral part of power converters and inverters, β-Ga_2O_3 Schottky barrier diodes (SBDs) have been intensively studied and undergone rapid progress. The majority of β-Ga_2O_3 SBDs reported in the literature are vertical devices. Thanks to the availability of native β-Ga_2O_3 substrates with low dislocation density, thick β-Ga_2O_3 drift layers with low background carrier concentration can be grown homoepitaxially[11–16]. Compared with a lateral configuration, the breakdown voltage (V_{br}) of vertical SBDs scales with the drift layer thickness as opposed to a lateral anode–to–cathode separation, which translates into a higher power density or a higher blocking voltage without sacrificing chip area. In addition, heat distribution is more uniform in vertical devices because of current spreading. Realization of the full potential of these devices requires proper edge termination designs that are suitable for implementation in β-Ga_2O_3 to limit the maximum electric field around the periphery of the rectifying contact.

β-Ga_2O_3 lacks p-type doping capability. This issue is fundamental to the material's electronic band structure[17–19]. The absence of definitive demonstrations of p-type doping in β-Ga_2O_3 renders bipolar homojunction diodes that are prevalent in other power device technologies impractical for this oxide semiconductor. To circumvent the challenge of developing p-type doping in β-Ga_2O_3 for edge termination, heterogeneous integration of β-Ga_2O_3 with other p-type oxide semiconductors has been proposed. Reactive-sputtered nickel oxide (NiO) has been widely adopted for forming p–n heterojunctions with β-Ga_2O_3 because of its relatively large bandgap (3.7 eV), relative ease of deposition with readily available toolsets, and propensity to exhibit native p-type conductivity tunable over several orders of magnitude through controlling deposition conditions.

This paper reviews a broad portfolio of β-Ga_2O_3 SBDs, the vast majority of which employ one or more edge-termination techniques to mitigate edge breakdown and enhance their power figure-of-merit (PFOM). The design and operating principles of advanced rectifier structures are then exam-

---

Correspondence to: M H Wong, eemhwong@ust.hk

Received 30 AUGUST 2023; Revised 16 SEPTEMBER 2023.

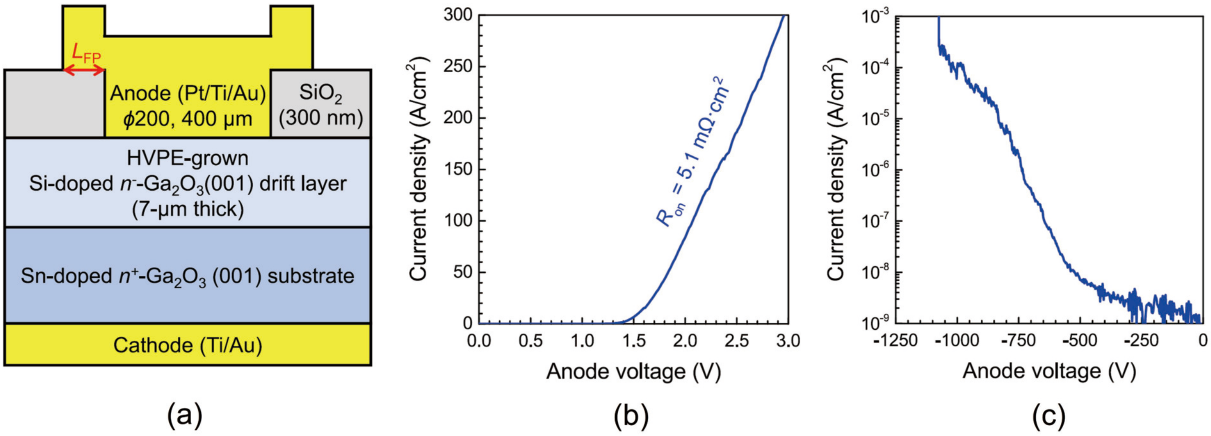

Fig. 1. (Color online) (a) Schematic of the first field-plated β-Ga_2O_3 SBD. (b) Forward current–voltage (I–V) characteristic of the device. (c) Reverse breakdown characteristic of the device. Reprinted from Ref. [21], with the permission of AIP Publishing.

ined. An assessment of β-Ga_2O_3 rectifier performance at elevated temperatures is provided toward the end.

2. Edge terminations for Schottky diodes

2.1. Field-plated SBDs

Field plating is a relatively simple edge-termination technique that makes use of a metal–insulator–semiconductor (MIS) capacitor structure located at the edge of the main device junction to modulate the local electric field[20]. Apart from a single-step field plate, which is the simplest field plate geometry, various other designs of field plates such as multistep and slanted geometries have been developed for high-voltage β-Ga_2O_3 SBDs. As a consequence of the simplicity and versatility of field plates, the literature contains an abundant documentation of field-plated β-Ga_2O_3 SBDs with a V_{br} higher than 1 kV (Fig. 1)[21−25]. Large-area field-plated devices have also been realized[26−31], with the highest reported forward current exceeding 100 A. However, the reverse leakage and V_{br} of large-area SBDs are typically worse than small-area devices of equivalent construction because of a higher probability of incorporating defects such as voids, dislocations, or polycrystalline inclusions within the active region[32−35].

2.2. SBDs with ultrahigh-permittivity dielectric engineering

The choice of dielectrics used for field plate termination structures profoundly affects the reverse V_{br} and leakage current of field-plated SBDs. To avoid accelerated dielectric degradation, the maximum field sustained by the dielectric should be limited to a value well below the threshold of catastrophic breakdown. Ultrahigh-permittivity dielectrics such as barium titanate and strontium titanate provide a new approach to edge termination for β-Ga_2O_3 power devices[36−40], whose high breakdown field calls for new methods of field management owing to a lack of dielectrics that can be stressed beyond the theoretical breakdown field of β-Ga_2O_3. These dielectrics are strongly polarizable by an external electric field, which induces internal dipoles and fixed surface charges in the dielectric material. When a reverse bias is applied to an ultrahigh-permittivity MIS capacitor associated with a field plate structure, the fringing electric field through the dielectric causes a lateral expansion of the depletion region in the semiconductor, thereby reducing the peak electric fields at the semiconductor surface. Furthermore, the induced polarization charges in the dielectric effectively screen both the positive donor charges in the semiconductor and the negative electron charges imaged in the anode metal. Thanks to this screening effect, the electric field in the ultrahigh-permittivity dielectric can be significantly lower than in the semiconductor, which leads to an increase in the effective barrier width for electron tunneling from the metal to the semiconductor. Achievements of a parallel-plane electric field of 5.7 MV/cm and a PFOM of 1.47 GW/cm^2—the first >1 GW/cm^2 demonstration for a unipolar vertical β-Ga_2O_3 device—highlight the efficacy of ultrahigh-permittivity dielectrics in enabling efficient edge termination and pushing the performance of β-Ga_2O_3 power devices toward intrinsic critical limits (Fig. 2)[39, 40].

2.3. Mesa-terminated SBDs

The field-crowding effect at the edge of an SBD can be relaxed by removing materials around the device edge to form a mesa structure such that the depletion region can be terminated on the exposed sidewall of the mesa. Junction curvature at the device edge is inherently relieved or eliminated, allowing more uniform distribution of electric field within the device. A deep etch is most effective when etching is past the maximum depletion layer thickness for non-punch-through breakdown or the drift layer thickness for punch-through breakdown; in both cases, electric field is prevented from developing at the mesa foot, hence avoiding premature breakdown even with steep (~90°) mesa profiles[41, 42]. Alternatively, beveled mesas characterized by an inclined sidewall and a bevel angle at the mesa foot can be implemented. With sufficiently small bevel angles, these structures enable effective edge termination without a need for deep etching beyond the depletion boundary at the rated V_{br}[43]. A bevel angle as small as ~1° has been fabricated (Fig. 3)[44]. In the forward conduction mode, the beveled geometry is advantageous for facilitating current spreading and enhancing current density. A dielectric is often deposited over the entire mesa structure after etching to passivate surface trap states caused by etch damage so as to mitigate parasitic leakage currents and ensure long-term device reliability.

2.4. SBDs with resistive termination

The concept of resistive edge termination is based upon the introduction of a nominally insulating or intrinsic layer in

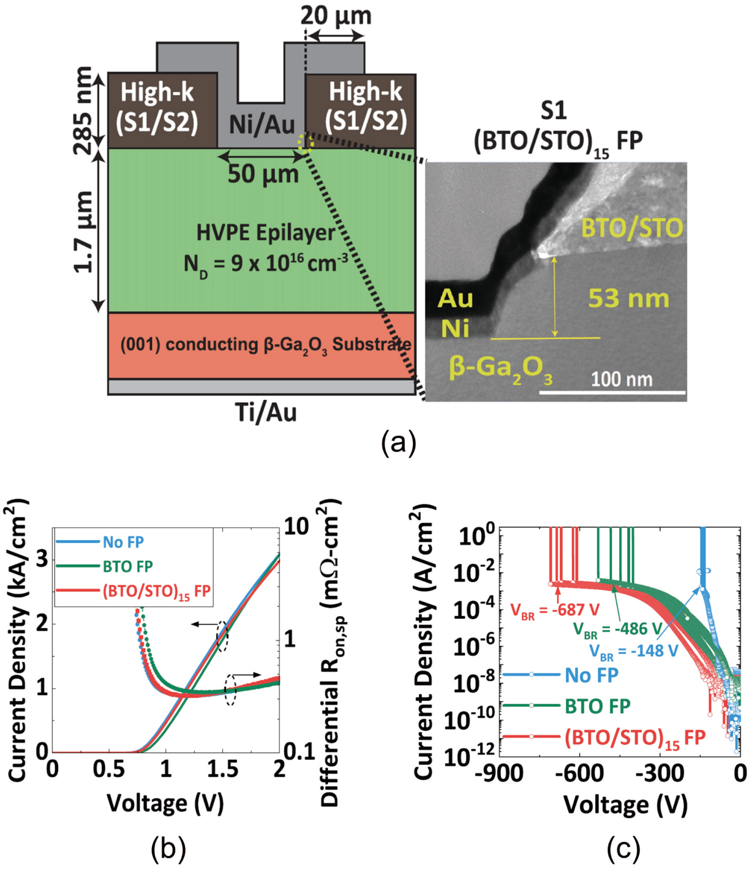

(a)

(b) (c)

Fig. 2. (Color online) (a) Schematic of a β-Ga_2O_3 SBD with an ultrahigh-permittivity field-plate dielectric, where S1 corresponds to a 15-period $BaTiO_3/SrTiO_3$ superlattice as the field-plate oxide [$(BTO/STO)_{15}$ FP] and S2 corresponds to $BaTiO_3$ as the field-plate oxide (BTO FP). The cross-sectional transmission electron microscopy image depicts the field-plated region of the S1 structure. (b) Forward *I*–*V* characteristics and differential $R_{ON,sp}$ of a β-Ga_2O_3 SBD with $(BTO/STO)_{15}$ FP, a β-Ga_2O_3 SBD with BTO FP, and a reference SBD without a field plate. (c) Reverse breakdown characteristics of the three different SBD structures. © 2021 IEEE. Reprinted, with permission, from Ref. [40].

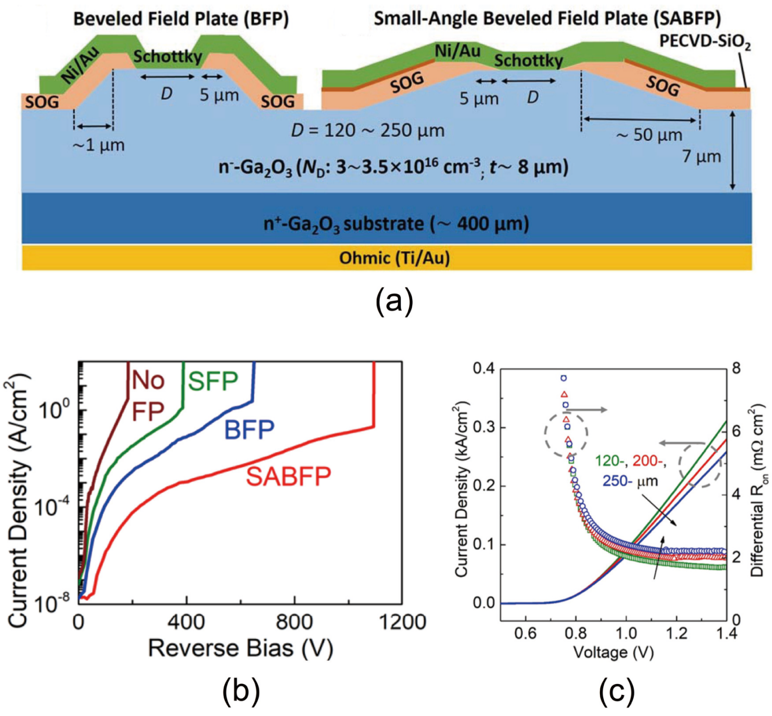

(a)

(b) (c)

Fig. 3. (Color online) (a) Schematics of beveled-mesa β-Ga_2O_3 SBDs with a ~45° beveled field plate (BFP) and with a small-angle (~1°) beveled field plate (SABFP). (b) Reverse breakdown characteristics of the BFP-SBD and SABFP-SBD showing higher V_{br} than those of mesa-free β-Ga_2O_3 SBDs that are either unterminated or terminated with a ~45° beveled surface field plate (SFP). (c) Forward *I*–*V* characteristics and differential $R_{ON,sp}$ of SABFP-SBDs with different anode diameters. © 2019 IEEE. Reprinted, with permission, from Ref. [44].

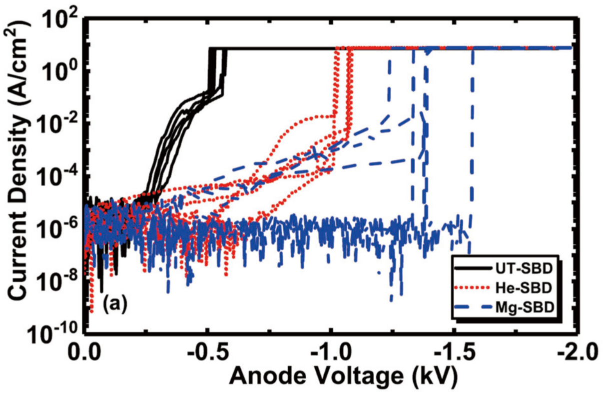

Fig. 4. (Color online) Comparison between reverse breakdown characteristics of β-Ga_2O_3 SBDs with no edge termination, He-implanted edge termination, and Mg-implanted edge termination. © 2020 IEEE. Reprinted, with permission, from Ref. [45].

contact with the anode periphery to spread the electric field by fringing. Resistive layers in β-Ga_2O_3 SBDs are commonly formed by ion implantation, which creates intrinsic defects via high-dose ion bombardment of either an inert species (e.g. He[45] or Ar[46, 47]) or a deep-level impurity (e.g. Mg[45, 48] or N[49, 50]) to form trap levels in the bandgap (Fig. 4). Resistive termination structures have also been implemented by etching a deep trench under the periphery of the Schottky contact and backfilling it with an insulating dielectric material like SiO_2[25, 51]. Thermal annealing of n-type β-Ga_2O_3 in oxygen is known to deplete or reduce carriers over a finite volume underneath the surface[16, 52, 53], an effect exploited to fabricate resistive edge-termination structures in β-Ga_2O_3 SBDs[54–56]. Through a combination of large V_{br} due to efficient termination and low specific on-resistance ($R_{ON,sp}$) due to high-quality epitaxy, a PFOM of up to 10.6 GW/cm^2 that exceeds the 1-D unipolar limits of SiC and GaN has been realized in SBDs employing resistive termination[51].

2.5. SBDs with fixed-charge termination

Fixed negative charges can be introduced, via plasma exposure or otherwise, to the surface of an n-type drift layer at the junction periphery to expand the depletion region along the surface from the main blocking junction, thus modifying the surface electric field and alleviating potential crowding at the junction periphery. Surface doping of β-Ga_2O_3 with fluoride ions for edge termination has been demonstrated via high-power CF_4 plasma exposure (Fig. 5)[57]. In addition to the negative fixed charge model, the effect of fluorine has also been conjectured to arise from compensation of positively ionized Si donors via the formation of neutral complexes[58], and may thus be regarded as a type of resistive termination. Plasma treatment inflicts much lower damage than mesa etching or ion implantation. Determination of the optimal charge profile for a given device structure requires systematic simulations that consider the thickness and doping of the drift layer, the lateral extension of the termination region, as well as the rated voltage of the device.

2.6. Junction-terminated SBDs

2.6.1. Guard rings and junction termination extension

Schottky power rectifiers can be edge terminated by incorporating a highly doped guard ring to create a p–n junction that overlaps the edge of the Schottky metal, thereby completely screening the metal edge from high electric fields. Typical implementations of this approach in β-Ga_2O_3 make use of p-NiO to form the guard ring[59]. Another p-type material option is the group-Ⅲ nitride semiconductor in view of the prospects of high-quality Ⅲ-nitride epitaxy on β-Ga_2O_3. Simulations of hybrid p-AlGaN/β-Ga_2O_3 devices have predicted very promising performance that awaits experimental validation[60].

The efficiency of highly doped, single-layer termination such as the guard ring is known to be sensitive to the charge density of the p-type layer. To realize broad design window and process latitude, advanced junction termination structures make use of multiple p-NiO layers with various lengths and acceptor densities to allow for a graded decrease in effective charge density away from the device active region while forming an extended depletion region at the device periphery[61, 62]. At breakdown, the p-NiO is fully depleted to balance the charge in the β-Ga_2O_3 drift layer.

2.6.2. Field-limiting rings

The concept of field-limiting rings (FLRs) for terminating a Schottky rectifier involves surrounding the main blocking junction by one or more isolated concentric ring junctions that are either Schottky or p–n (Fig. 6)[63]. When the rectifier is under the blocking condition, this ring system reduces the amount of field crowding at the main junction by spreading the depletion layer consecutively past the ring junctions that are typically left floating. FLR termination of β-Ga_2O_3 SBDs is first demonstrated experimentally using mechanically exfoliated β-Ga_2O_3 flakes[64]. For higher voltage ratings, multiple rings are required to provide a V_{br} close to the parallel-plane limit, whereby the electric field developed at the edge of a floating ring can be reduced by the addition of another floating ring. Judicious biasing of the FLRs can improve the termination efficiency owing to reduced sensitivity of the biased structure to the inter-ring distance and the additional control over breakdown [65].

3. Junction barrier Schottky diodes and trench Schottky barrier diodes

SBDs typically display soft breakdown characteristics. At high reverse bias, Schottky barrier lowering due to the image-force effect results in large tunneling and thermionic emission currents that limit the breakdown of SBDs to voltages much smaller than the 1-D parallel-plane value even if edge effects are eliminated[66]. Consequently, the rated V_{br} is determined by the maximum allowable leakage current instead of avalanche breakdown. The constraint imposed by high leakage current renders the effective PFOM of regular SBDs much lower than the projected theoretical limit of the semiconductor. Such discrepancy exacerbates for ultrawide-bandgap semiconductors like β-Ga_2O_3. While it is possible to approach the intrinsic E_{cr} of 6–8 MV/cm in β-Ga_2O_3 SBDs with a sufficiently large Schottky barrier (2.2–3 eV) (Fig. 7)[67], reducing the leakage current by increasing the Schottky barrier height comes with the penalty of a higher turn-on voltage (V_{ON}). To obtain a large V_{br} without increasing the barrier height, the leakage needs to be decoupled from the reverse-bias voltage such that the maximum electric field is transferred from the Schottky interface to within the device body.

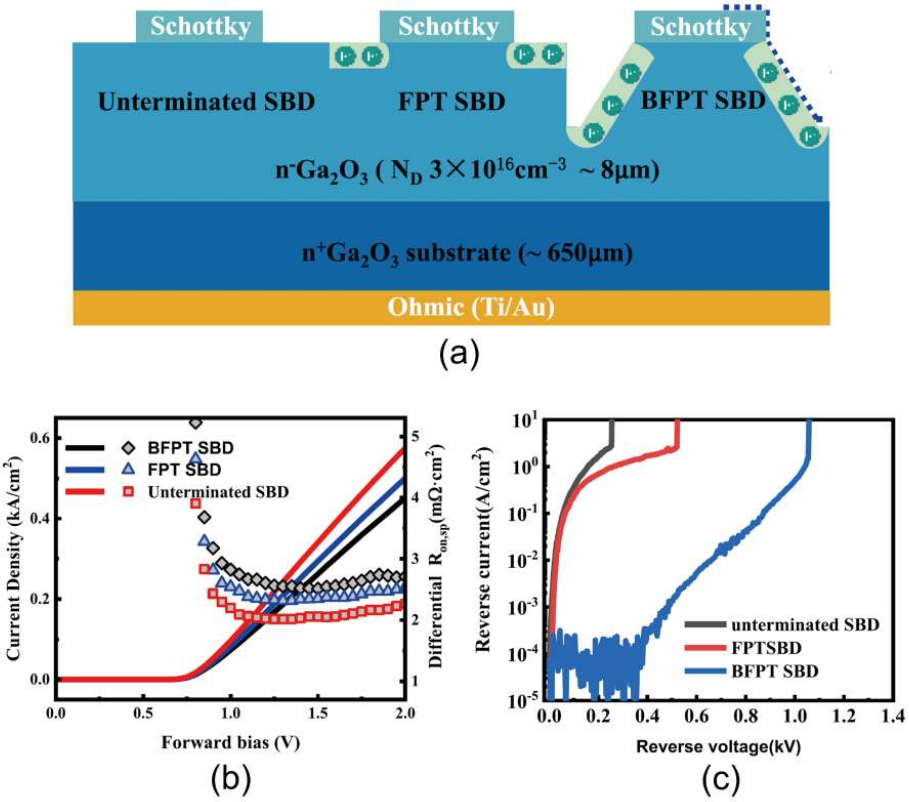

(a)

(b)

(c)

Fig. 5. (Color online) Schematics of an unterminated β-Ga_2O_3 SBD, a β-Ga_2O_3 SBD with self-aligned fluorine plasma treatment (FPT), and a β-Ga_2O_3 SBD with self-aligned beveled fluorine plasma treatment (BFPT). (b) Forward I–V characteristics and differential $R_{ON,sp}$ of the three different SBDs. (c) Reverse breakdown characteristics of the three different SBDs. © 2020 IEEE. Reprinted, with permission, from Ref. [57].

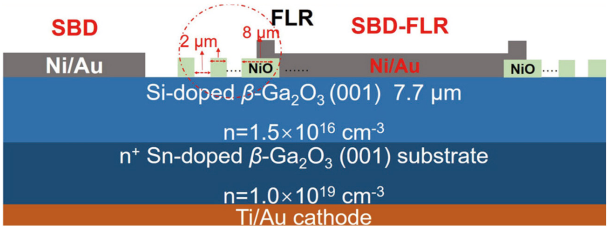

Fig. 6. (Color online) Schematic of a β-Ga_2O_3 SBD terminated with p-NiO FLRs alongside an unterminated device. Reprinted from Ref. [63], with the permission of AIP Publishing.

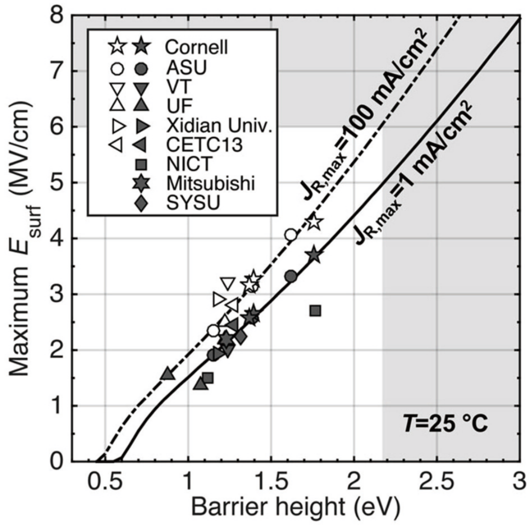

Fig. 7. Calculated maximum surface electric fields (E_{surf}) in β-Ga_2O_3 SBDs, defined at a maximum reverse leakage current ($J_{R,max}$) of 1 or 100 mA/cm^2 at 25 °C. Experimental data from the literature are also shown (solid for $J_{R,max}$ = 1 mA/cm^2 and hollow for $J_{R,max}$ = 100 mA/cm^2). Adapted from Ref. [67], with the permission of AIP Publishing.

The aforementioned electric-field profile can be achieved by embedding p–n junctions under the Schottky contact as a screen to lower the surface electric field during reverse bias[68–70], in a device structure known as the junction barrier Schottky diode (JBSD). The reduced-surface-field (RESURF) effect due to charge coupling between the p$^+$ regions and the n$^-$ drift layer in JBSDs effectively minimizes Schottky barrier lowering and enables the JBSD structure to exhibit the low reverse leakage current of a p–n diode. Furthermore, one can capitalize on the RESURF effect to reduce the $R_{ON,sp}$ and thus the power loss of a JBSD since the surface electric field at breakdown can be lower than the maximum electric field in the drift layer, which allows for higher doping in the drift layer for a given voltage rating. For UWBG semiconductors like β-Ga_2O_3, it is even more important to utilize the RESURF effect for medium- to high-voltage rectifiers owing to the large difference between E_{cr} and the leakage-limited practical maximum surface field. With effective native p-type doping remaining elusive in β-Ga_2O_3, researchers have sought to realize β-Ga_2O_3 JBSD structures based on p-NiO/n-Ga_2O_3 heterojunctions. JBSDs showing several orders of magnitude smaller leakage current with no or insignificant penalty on V_{ON} and $R_{ON,sp}$ compared with a cofabricated regular SBD serve as a clear proof of concept for the RESURF effect (Fig. 8)[63, 71–74].

The periodic array of p–n junctions in a JBSD can be replaced with nonplanar MOS structures constructed in an

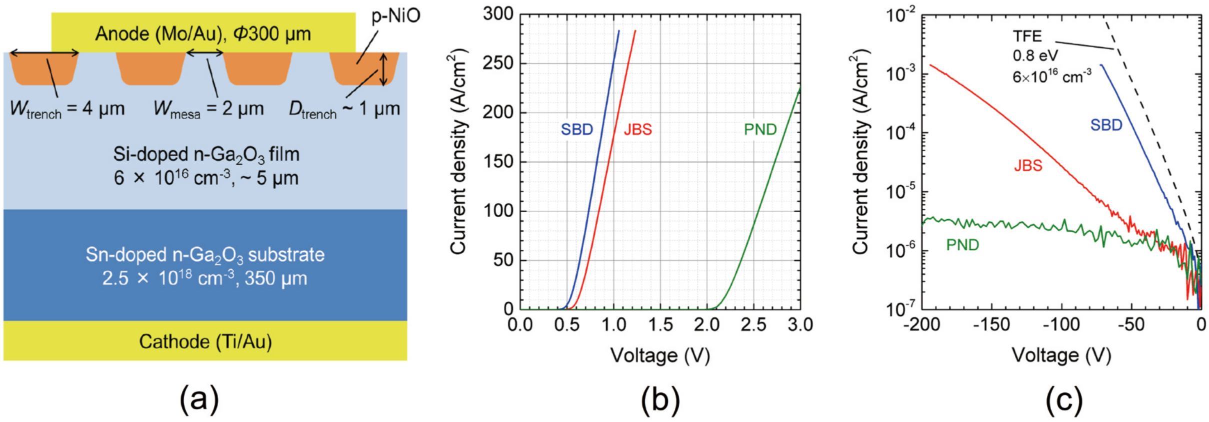

Fig. 8. (Color online) (a) Schematic of the first β-Ga_2O_3 JBSD. (b) Forward I–V characteristic of the JBSD showing similar V_{ON} to a regular β-Ga_2O_3 SBD and lower V_{ON} than a p-NiO/n-Ga_2O_3 diode (PND). (c) Reverse breakdown characteristic of the JBSD showing higher V_{br} than a regular β-Ga_2O_3 SBD because of the RESURF effect but lower V_{br} than a PND owing to higher reverse leakage current through a Schottky junction. Reprinted with permission from Ref. [72]. Copyright 2019 SPIE.

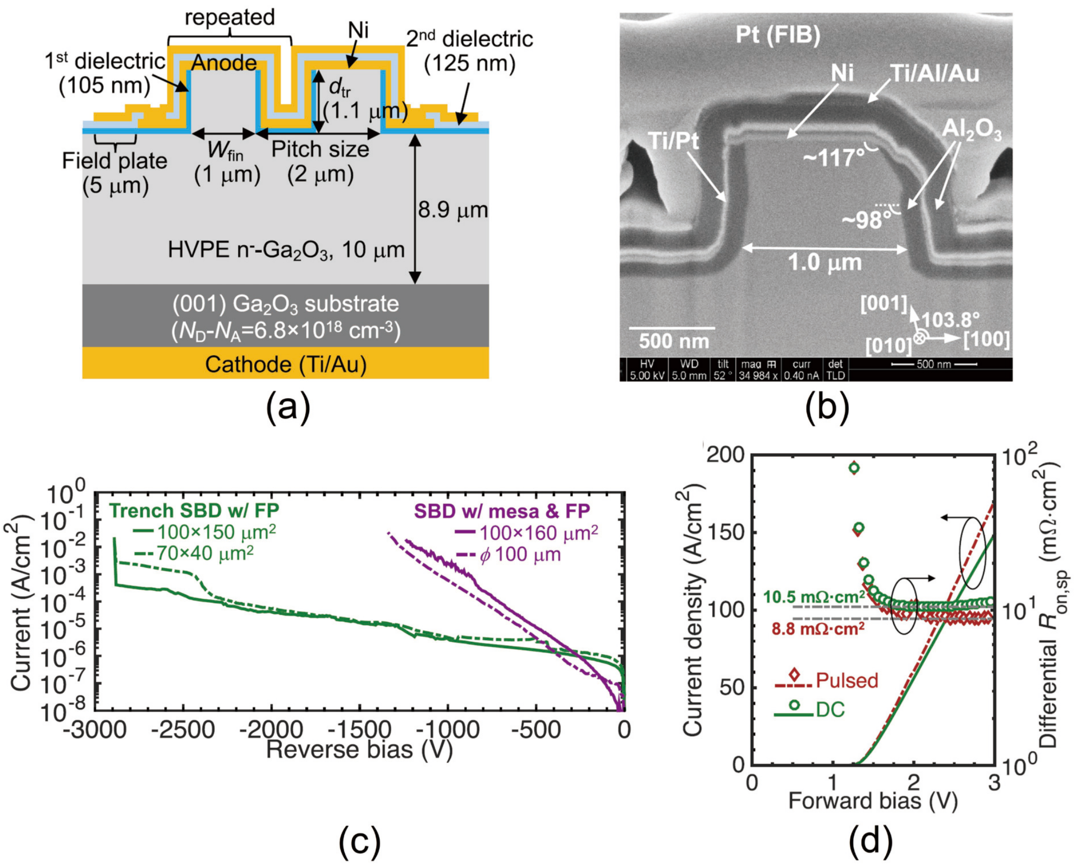

Fig. 9. (Color online) (a) Schematic of a field-plated β-Ga_2O_3 trench SBD. (b) Cross-sectional scanning electron microscopy image of a fin channel. (c) Reverse breakdown characteristics of field-plated β-Ga_2O_3 trench SBDs. In comparison with regular β-Ga_2O_3 SBDs employing both mesa and field plate terminations, the field-plated trench devices have much lower leakage current and a much higher V_{br}. (d) Forward I–V characteristics and differential $R_{ON,sp}$ of field-plated β-Ga_2O_3 trench SBDs under DC and pulsed conditions. A base voltage of 0 V, a pulse width of 1 μs, and a duty cycle of 0.1% are used for the pulsed measurements. © 2020 IEEE. Reprinted, with permission, from Ref. [82].

alternating fin/trench geometry (Fig. 9) [75–83]. By virtue of the RESURF effect, the reverse leakage current in trench SBDs is generally much lower than in regular SBDs at destructive breakdown. The RESURF effect can be controlled through optimizations of the fin/trench geometry (fin width, trench depth, pitch size) to satisfy design constraints on $R_{ON,sp}$, reverse leakage, and maximum electric fields (Fig. 10). However, the RESURF effect also leads to enhanced electric fields at the bottom corners and the center of the trenches, the former of which can be managed by increasing the corner radius[84]. Orientation of the fin is found to have a strong influence on the forward conduction[85], where sidewall interface trapping is found to cause current collapse and delayed turn-on due to sidewall depletion[86]. To mitigate the sidewall trapping effects, wet acid treatments are performed to reduce the etch-induced damage and smooth the fin sidewalls.

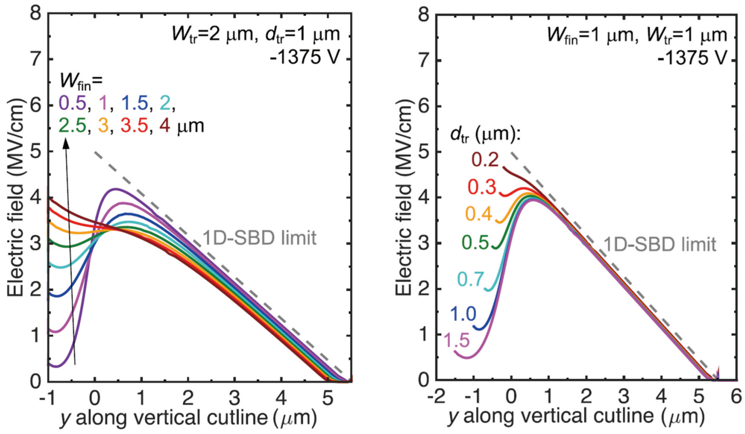

(a) (b)

Fig. 10. (Color online) Simulated electric-field profiles in a β-Ga_2O_3 trench SBD along a vertical cutline at the center of a fin under a reverse bias of −1375 V by varying (a) fin width [W_{fin}, see Fig. 9(a)] and (b) trench depth [d_{tr}, see Fig. 9(a)]. © 2020 IEEE. Reprinted, with permission, from Ref. [83].

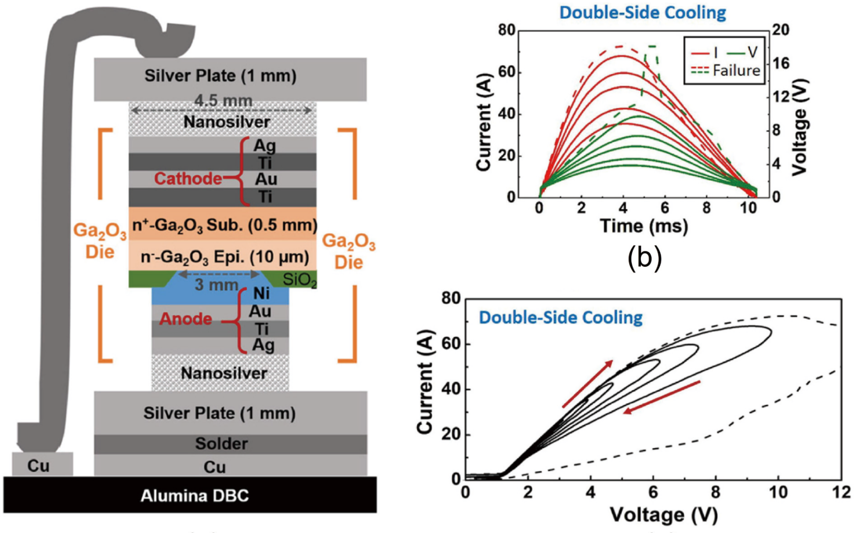

(a) (b) (c)

Fig. 11. (Color online) (a) Schematic of a field-plated β-Ga_2O_3 SBD with double-side-cooling flip-chip package. (b) I–V waveforms of the double-side-cooled device in surge current tests. (c) I–V loops of the double-side-cooled device. © 2021 IEEE. Reprinted, with permission, from Ref. [90].

4. High-temperature performance of β-Ga_2O_3 Schottky diodes

β-Ga_2O_3 rectifiers are attractive for high-temperature applications by virtue of their significantly lower intrinsic carrier density than in Si, SiC, and GaN. High-temperature operation at 500 °C has been demonstrated[87, 88]. Unique challenges arise from the device-level thermal resistance due to the low thermal conductivity of β-Ga_2O_3. It has been found that packaging strategies involving junction-side or flip-chip cooling as well as double-side cooling are the most effective. Thin-body rectifiers that are flip-chip packaged have achieved a high surge current of 59 A[89]. Double-side-cooled β-Ga_2O_3 SBDs have been shown to be capable of sustaining a peak surge current over 60 A (Fig. 11), with a ratio between the peak surge current and the rated current superior to that of similarly rated commercial SiC SBDs[90, 91]. Trench SBDs of β-Ga_2O_3 have also shown fascinating thermal stability[92, 93]. The resilience of β-Ga_2O_3 SBDs against high surge current is attributed to two key mechanisms[91]. First, the power-law temperature dependence of the $R_{ON,sp}$ in β-Ga_2O_3 devices shows a temperature coefficient 2 to 4 times smaller than the corresponding values of SiC SBDs. This is possibly due to a weak temperature dependence of electron mobility in β-Ga_2O_3 and an increase in donor ionization at high temperatures[94], both reducing the risk of thermal runaway. Second, the double-side and flip-chip packaging strategies allow heat extraction directly from the Schottky junction rather than through the thermally resistive β-Ga_2O_3 substrate. It is noteworthy that impact ionization breakdown of β-Ga_2O_3 was recently demonstrated, albeit in a p-NiO/n-Ga_2O_3 heterojunction instead of an SBD[95]. Avalanche capability imparts surge robustness to β-Ga_2O_3 devices by enabling effective dissipation of the surge energy.

5. Conclusions

β-Ga_2O_3 SBDs have demonstrated favorable attributes to be the next frontier in power electronic devices. These achievements benefit from the excellent quality of homoepitaxial growth on native substrates with low dislocation density. Various types of edge termination methods have been implemented for field management to effectively harness the high

E_{cr} afforded by β-Ga_2O_3. To this end, there have been applications of p-type NiO for edge termination in β-Ga_2O_3 SBDs and for constructing β-Ga_2O_3 JBSD structures. The p-NiO/n-Ga_2O_3 heterojunction p–n diode is also attractive in its own right and has shown exemplary performance as a standalone power device[96−100]. By employing an optimized junction termination extension scheme, the PFOM for heterojunction diodes with a V_{br} of 3.3 kV exceeds 2.5 GW/cm^2, which surpasses the 1-D SiC limit and is among the highest in multi-kilovolt β-Ga_2O_3 rectifiers[100]. In JBSD and trench SBD structures, the maximum electric field is transferred from the Schottky interface to within the bulk of the drift layer thanks to the RESURF effect, which allows the field to be decoupled from the reverse leakage current, thus reducing the optimal $R_{ON,sp}$ and improving the PFOM. Along with field management, heat dissipation to limit the junction temperature and improve the component reliability is also critical for maximizing the performance of β-Ga_2O_3 power devices.

References

[1] Tsao J Y, Chowdhury S, Hollis M A, et al. Ultrawide-bandgap semiconductors: Research opportunities and challenges. Adv Electron Mater, 2018, 4, 1600501

[2] Slobodyan O, Flicker J, Dickerson J, et al. Analysis of the dependence of critical electric field on semiconductor bandgap. J Mater Res, 2022, 37, 849

[3] Higashiwaki M, Jessen G H. Guest Editorial: The dawn of gallium oxide microelectronics. Appl Phys Lett, 2018, 112, 060401

[4] Chabak K D, Leedy K D, Green A J, et al. Lateral β-Ga_2O_3 field effect transistors. Semicond Sci Technol, 2020, 35, 013002

[5] Wong M H, Higashiwaki M. Vertical β-Ga_2O_3 power transistors: A review. IEEE Trans Electron Devices, 2020, 67, 3925

[6] Ma N, Tanen N, Verma A, et al. Intrinsic electron mobility limits in β-Ga_2O_3. Appl Phys Lett, 2016, 109, 212101

[7] Reese S B, Remo T, Green J, et al. How much will gallium oxide power electronics cost? Joule, 2019, 3, 903

[8] Heinselman K N, Haven D, Zakutayev A, et al. Projected cost of gallium oxide wafers from edge-defined film-fed crystal growth. Cryst Growth Des, 2022, 22, 4854

[9] Hou X H, Zou Y N, Ding M F, et al. Review of polymorphous Ga_2O_3 materials and their solar-blind photodetector applications. J Phys D: Appl Phys, 2021, 54, 043001

[10] Zhou J G, Chen H, Fu K, et al. Gallium oxide-based optical nonlinear effects and photonics devices. J Mater Res, 2021, 36, 4832

[11] Murakami H, Nomura K, Goto K, et al. Homoepitaxial growth of β-Ga_2O_3 layers by halide vapor phase epitaxy. Appl Phys Express, 2015, 8, 015503

[12] Thieu Q T, Wakimoto D, Koishikawa Y, et al. Preparation of 2-in.-diameter (001) β-Ga_2O_3 homoepitaxial wafers by halide vapor phase epitaxy. Jpn J Appl Phys, 2017, 56, 110310

[13] Goto K, Konishi K, Murakami H, et al. Halide vapor phase epitaxy of Si doped β-Ga_2O_3 and its electrical properties. Thin Solid Films, 2018, 666, 182

[14] Leach J H, Udwary K, Rumsey J, et al. Halide vapor phase epitaxial growth of β-Ga_2O_3 and α-Ga_2O_3 films. APL Mater, 2019, 7, 022504

[15] Goto K, Murakami H, Kuramata A, et al. Effect of substrate orientation on homoepitaxial growth of β-Ga_2O_3 by halide vapor phase epitaxy. Appl Phys Lett, 2022, 120, 102102

[16] Kuramata A, Koshi K, Watanabe S, et al. High-quality β-Ga_2O_3 single crystals grown by edge-defined film-fed growth. Jpn J Appl Phys, 2016, 55, 1202A2

[17] Kyrtsos A, Matsubara M, Bellotti E. On the feasibility of p-type Ga_2O_3. Appl Phys Lett, 2018, 112, 032108

[18] Gake T, Kumagai Y, Oba F. First-principles study of self-trapped holes and acceptor impurities in Ga_2O_3 polymorphs. Phys Rev Materials, 2019, 3, 044603

[19] Varley J B, Janotti A, Franchini C, et al. Role of self-trapping in luminescence and p-type conductivity of wide-band-gap oxides. Phys Rev B, 2012, 85, 081109

[20] Grove A S, Leistiko O, Hooper W W. Effect of surface fields on the breakdown voltage of planar silicon p-n junctions. IEEE Trans Electron Devices, 1967, 14, 157

[21] Konishi K, Goto K, Murakami H, et al. 1-kV vertical Ga_2O_3 field-plated Schottky barrier diodes. Appl Phys Lett, 2017, 110, 103506

[22] Hu Z Z, Zhou H, Feng Q, et al. Field-plated lateral β-Ga_2O_3 Schottky barrier diode with high reverse blocking voltage of more than 3 kV and high DC power figure-of-merit of 500 MW/cm^2. IEEE Electron Device Lett, 2018, 39, 1564

[23] Yang J C, Ren F, Tadjer M, et al. 2300V reverse breakdown voltage Ga_2O_3 Schottky rectifiers. ECS J Solid State Sci Technol, 2018, 7, Q92

[24] Chen Y T, Yang J C, Ren F, et al. Implementation of a 900V switching circuit for high breakdown voltage β-Ga_2O_3 Schottky diodes. ECS J Solid State Sci Technol, 2019, 8, Q3229

[25] Kumar S, Murakami H, Kumagai Y, et al. Vertical β-Ga_2O_3 Schottky barrier diodes with trench staircase field plate. Appl Phys Express, 2022, 15, 054001

[26] Yang J C, Ren F, Tadjer M, et al. Ga_2O_3 Schottky rectifiers with 1 ampere forward current, 650 V reverse breakdown and 26.5 MW•cm^{-2} figure-of-merit. AIP Adv, 2018, 8, 055026

[27] Yang J C, Ren F, Pearton S J, et al. Vertical geometry, 2-A forward current Ga_2O_3 Schottky rectifiers on bulk Ga_2O_3 substrates. IEEE Trans Electron Devices, 2018, 65, 2790

[28] Yang J C, Xian M H, Carey P, et al. Vertical geometry 33.2 A, 4.8 MW cm^{-2} Ga_2O_3 field-plated Schottky rectifier arrays. Appl Phys Lett, 2019, 114, 232106

[29] Yang J C, Fares C, Elhassani R, et al. Reverse breakdown in large area, field-plated, vertical β-Ga_2O_3 rectifiers. ECS J Solid State Sci Technol, 2019, 8, Q3159

[30] Ji M, Taylor N R, Kravchenko I, et al. Demonstration of large-size vertical Ga_2O_3 Schottky barrier diodes. IEEE Trans Power Electron, 2020, 36, 41

[31] Sharma R, Xian M H, Fares C, et al. Effect of probe geometry during measurement of >100 A Ga_2O_3 vertical rectifiers. J Vac Sci Technol A, 2021, 39, 013406

[32] Kasu M, Hanada K, Moribayashi T, et al. Relationship between crystal defects and leakage current in β-Ga_2O_3 Schottky barrier diodes. Jpn J Appl Phys, 2016, 55, 1202BB

[33] Oshima T, Hashiguchi A, Moribayashi T, et al. Electrical properties of Schottky barrier diodes fabricated on (001) β-Ga_2O_3 substrates with crystal defects. Jpn J Appl Phys, 2017, 56, 086501

[34] Sdoeung S, Sasaki K, Kawasaki K, et al. Origin of reverse leakage current path in edge-defined film-fed growth (001) β-Ga_2O_3 Schottky barrier diodes observed by high-sensitive emission microscopy. Appl Phys Lett, 2020, 117, 022106

[35] Sdoeung S, Sasaki K, Kawasaki K, et al. Polycrystalline defects—Origin of leakage current—In halide vapor phase epitaxial (001) β-Ga_2O_3 Schottky barrier diodes identified via ultrahigh sensitive emission microscopy and synchrotron X-ray topography. Appl Phys Express, 2021, 14, 036502

[36] Xia Z B, Wang C Y, Kalarickal N K, et al. Design of transistors using high-permittivity materials. IEEE Trans Electron Devices, 2019, 66, 896

[37] Lee H-S, Kalarickal N K, Rahman M W, et al. High-permittivity dielectric edge termination for vertical high voltage devices. J Comput Electron, 2020, 19, 1538

[38] Kalarickal N K, Feng Z X, Bhuiyan A F M A U, et al. Electrostatic

engineering using extreme permittivity materials for ultra-wide bandgap semiconductor transistors. IEEE Trans Electron Devices, 2021, 68, 29

[39] Xia Z B, Chandrasekar H, Moore W, et al. Metal/$BaTiO_3$/β-Ga_2O_3 dielectric heterojunction diode with 5.7 MV/cm breakdown field. Appl Phys Lett, 2019, 115, 252104

[40] Roy S, Bhattacharyya A, Ranga P, et al. High-k oxide field-plated vertical (001) β-Ga_2O_3 Schottky barrier diode with baliga's figure of merit over 1 GW/cm^2. IEEE Electron Device Lett, 2021, 42, 1140

[41] Saraswat D, Li W S, Nomoto K, et al. Very high parallel-plane surface electric field of 4.3 MV/cm in Ga_2O_3 Schottky barrier diodes with PtO_x contacts. 2020 78th Device Research Conference (DRC), 2020, 1

[42] Farzana E, Alema F, Ho W Y, et al. Vertical β-Ga_2O_3 field plate Schottky barrier diode from metal-organic chemical vapor deposition. Appl Phys Lett, 2021, 118, 162109

[43] Joishi C, Rafique S, Xia Z B, et al. Low-pressure CVD-grown β-Ga_2O_3 bevel-field-plated Schottky barrier diodes. Appl Phys Express, 2018, 11, 031101

[44] Allen N, Xiao M, Yan X D, et al. Vertical Ga_2O_3 Schottky barrier diodes with small-angle beveled field plates: A Baliga's figure-of-merit of 0.6 GW/cm^2. IEEE Electron Device Lett, 2019, 40, 1399

[45] Zhang Y N, Zhang J C, Feng Z Q, et al. Impact of implanted edge termination on vertical β-Ga_2O_3 Schottky barrier diodes under OFF-state stressing. IEEE Trans Electron Devices, 2020, 67, 3948

[46] Lu X, Zhang X, Jiang H X, et al. Vertical β-Ga_2O_3 Schottky barrier diodes with enhanced breakdown voltage and high switching performance. Phys Status Solidi A, 2020, 217, 1900497

[47] Gao Y Y, Li A, Feng Q, et al. High-voltage β-Ga_2O_3 Schottky diode with argon-implanted edge termination. Nanoscale Res Lett, 2019, 14, 8

[48] Zhou H, Yan Q L, Zhang J C, et al. High-performance vertical β-Ga_2O_3 Schottky barrier diode with implanted edge termination. IEEE Electron Device Lett, 2019, 40, 1788

[49] Xia X Y, Xian M H, Fares C, et al. Nitrogen ion-implanted resistive regions for edge termination of vertical Ga_2O_3 rectifiers. J Vac Sci Technol A, 2021, 39, 063405

[50] Lin C-H, Yuda Y, Wong M H, et al. Vertical Ga_2O_3 Schottky barrier diodes with guard ring formed by nitrogen-ion implantation. IEEE Electron Device Lett, 2019, 40, 1487

[51] Dong P F, Zhang J C, Yan Q L, et al. 6 kV/3.4 m$\Omega\cdot$cm^2 vertical β-Ga_2O_3 Schottky barrier diode with $BV^2/R_{on,sp}$ performance exceeding 1-D unipolar limit of GaN and SiC. IEEE Electron Device Lett, 2022, 43, 765

[52] Oshima T, Kaminaga K, Mukai A, et al. Formation of semi-insulating layers on semiconducting β-Ga_2O_3 single crystals by thermal oxidation. Jpn J Appl Phys, 2013, 52, 051101

[53] Swain S K, Weber M H, Jesenovec J, et al. Compensation of shallow donors by gallium vacancies in monoclinic β-Ga_2O_3. Phys Rev Applied, 2021, 15, 054010

[54] Wang Y G, Lv Y J, Long S B, et al. High-voltage ($\bar{2}01$) β-Ga_2O_3 vertical Schottky barrier diode with thermally-oxidized termination. IEEE Electron Device Lett, 2020, 41, 131

[55] Wang Y G, Lv Y J, Dun S B, et al. High performance β-Ga_2O_3 vertical Schottky barrier diodes. 2020 17th China International Forum on Solid State Lighting & 2020 6th International Forum on Wide Bandgap Semiconductors China, 2020, 224

[56] Wei Y X, Luo X R, Wang Y G, et al. Experimental study on static and dynamic characteristics of Ga_2O_3 Schottky barrier diodes with compound termination. IEEE Trans Power Electron, 2021, 36, 10976

[57] Hu Z Z, Lv Y J, Zhao C Y, et al. Beveled fluoride plasma treatment for vertical β-Ga_2O_3 Schottky barrier diode with high reverse blocking voltage and low turn-on voltage. IEEE Electron Device Lett, 2020, 41, 441

[58] Yang J C, Fares C, Ren F, et al. Effects of fluorine incorporation into β-Ga_2O_3. J Appl Phys, 2018, 123, 441

[59] Yan Q L, Gong H H, Zhou H, et al. Low density of interface trap states and temperature dependence study of Ga_2O_3 Schottky barrier diode with p-NiO_x termination. Appl Phys Lett, 2022, 120, 092106

[60] Roy S, Bhattacharyya A, Krishnamoorthy S. Design of a β-Ga_2O_3 Schottky barrier diode with p-type III-nitride guard ring for enhanced breakdown. IEEE Trans Electron Devices, 2020, 67, 4842

[61] Wang B Y, Xiao M, Spencer J, et al. 2.5 kV vertical Ga_2O_3 Schottky rectifier with graded junction termination extension. IEEE Electron Device Lett, 2023, 44, 221

[62] Hao W B, Wu F H, Li W S, et al. Improved vertical β-Ga_2O_3 Schottky barrier diodes with conductivity-modulated p-NiO junction termination extension. IEEE Trans Electron Devices, 2023, 70, 2129

[63] Gong H H, Yu X X, Xu Y, et al. β-Ga_2O_3 vertical heterojunction barrier Schottky diodes terminated with p-NiO field limiting rings. Appl Phys Lett, 2021, 118, 202102

[64] Hu Z, Zhao C, Feng Q, et al. The investigation of β-Ga_2O_3 Schottky diode with floating field ring termination and the interface states. ECS J Solid State Sci Technol, 2020, 9(2), 025001

[65] Sharma R, Xian M H, Law M E, et al. Design and implementation of floating field ring edge termination on vertical geometry β-Ga_2O_3 rectifiers. J Vac Sci Technol A, 2020, 38, 063414

[66] Rhoderick E H. Metal-semiconductor contacts. IEE Proceedings I (Solid-State and Electron Devices), 1982, 129, 1.

[67] Li W S, Saraswat D, Long Y Y, et al. Near-ideal reverse leakage current and practical maximum electric field in β-Ga_2O_3 Schottky barrier diodes. Appl Phys Lett, 2020, 116, 192101

[68] Wilamowski B M. Schottky diodes with high breakdown voltages. Solid State Electron, 1983, 26, 491

[69] Baliga B J. The pinch rectifier: A low-forward-drop high-speed power diode. IEEE Electron Device Lett, 1984, 5, 194

[70] Baliga B J. Analysis of a high-voltage merged p-i-n/Schottky (MPS) rectifier. IEEE Electron Device Lett, 1987, 8, 407

[71] Sasaki K, Thieu Q T, Wakimoto D, et al. First demonstration of Ga_2O_3 junction barrier Schottky diodes. 2017 17th International Conference on Silicon Carbide and Related Materials (ICSCRM), 2017, WE.E1.7

[72] Sasaki K, Yamakoshi S, Kuramata A. Gallium-oxide trench-type devices. Proc SPIE, 2019, 10919, 1091913

[73] Yan Q L, Gong H H, Zhang J C, et al. β-Ga_2O_3 hetero-junction barrier Schottky diode with reverse leakage current modulation and $BV^2/R_{on,sp}$ value of 0.93 GW/cm^2. Appl Phys Lett, 2021, 118, 122102

[74] Lv Y J, Wang Y G, Fu X C, et al. Demonstration of β-Ga_2O_3 junction barrier Schottky diodes with a Baliga's figure of merit of 0.85 GW/cm^2 or a 5A/700 V handling capabilities. IEEE Trans Power Electron, 2021, 36, 6179

[75] Sasaki K, Wakimoto D, Thieu Q T, et al. First demonstration of Ga_2O_3 trench MOS-type Schottky barrier diodes. IEEE Electron Device Lett, 2017, 38, 783

[76] Takatsuka A, Sasaki K, Wakimoto D, et al. Fast recovery performance of β-Ga_2O_3 trench MOS Schottky barrier diodes. 2018 76th Device Research Conference (DRC), 2018, 1

[77] Otsuka F, Miyamoto H, Takatsuka A, et al. Large-size (1.7 × 1.7 mm^2 β-Ga_2O_3 field-plated trench MOS-type Schottky barrier diodes with 1.2 kV breakdown voltage and 10^9 high on/off current ratio. Appl Phys Express, 2022, 15, 016501

[78] Li W S, Nomoto K, Hu Z Y, et al. 1.5 kV vertical Ga_2O_3 trench-MIS Schottky barrier diodes. 2018 76th Device Research Conference (DRC), 2018, 1

[79] Li W S, Hu Z Y, Nomoto K, et al. 1230 V β-Ga_2O_3 trench Schottky barrier diodes with an ultra-low leakage current of 1 μA/cm^2. Appl Phys Lett, 2018, 113, 202101

[80] Li W S, Hu Z Y, Nomoto K, et al. 2.44 kV Ga_2O_3 vertical trench Schottky barrier diodes with very low reverse leakage current. 2018 IEEE International Electron Devices Meeting (IEDM), 2018, 8.5. 1

[81] Li W S, Nomoto K, Hu Z Y, et al. Field-plated Ga_2O_3 trench Schottky barrier diodes with a record high figure-of-merit of 0.78 GW/cm^2. 2019 77th Device Research Conference (DRC), 2019, 1

[82] Li W S, Nomoto K, Hu Z Y, et al. Field-plated Ga_2O_3 trench Schottky barrier diodes with a $BV^2/R_{on,sp}$ of up to 0.95 GW/cm^2. IEEE Electron Device Lett, 2020, 41, 107

[83] Li W S, Nomoto K, Hu Z Y, et al. Guiding principles for trench Schottky barrier diodes based on ultrawide bandgap semiconductors: A case study in Ga_2O_3. IEEE Trans Electron Devices, 2020, 67, 3938

[84] Huang X A, Liao F, Li L, et al. 3.4 kV breakdown voltage Ga_2O_3 trench Schottky diode with optimized trench corner radius. ECS J Solid State Sci Technol, 2020, 9, 045012

[85] Li W S, Nomoto K, Hu Z Y, et al. Fin-channel orientation dependence of forward conduction in kV-class Ga_2O_3 trench Schottky barrier diodes. Appl Phys Express, 2019, 12, 061007

[86] Li W S, Nomoto K, Hu Z Y, et al. ON-resistance of Ga_2O_3 trench-MOS Schottky barrier diodes: Role of sidewall interface trapping. IEEE Trans Electron Devices, 2021, 68, 2420

[87] Fares C, Ren F, Pearton S J. Temperature-dependent electrical characteristics of β-Ga_2O_3 diodes with W Schottky contacts up to 500 °C. ECS J Solid State Sci Technol, 2018, 8, Q3007

[88] Hou C, York K R, Makin R A, et al. High temperature (500 °C) operating limits of oxidized platinum group metal (PtO_x, IrO_x, PdO_x, RuO_x) Schottky contacts on β-Ga_2O_3. Appl Phys Lett, 2020, 117, 203502

[89] Gong H H, Zhou F, Yu X X, et al. 70-μm-body Ga_2O_3 Schottky barrier diode with 1.48 K/W thermal resistance, 59 A surge current and 98.9% conversion efficiency. IEEE Electron Device Lett, 2022, 43, 773

[90] Xiao M, Wang B Y, Liu J C, et al. Packaged Ga_2O_3 Schottky rectifiers with over 60-A surge current capability. IEEE Trans Power Electron, 2021, 36, 8565

[91] Buttay C, Wong H Y, Wang B Y, et al. Surge current capability of ultra-wide-bandgap Ga_2O_3 Schottky diodes. Microelectron Reliab, 2020, 114, 113743

[92] Jian Z A, Mohanty S, Ahmadi E. Temperature-dependent current-voltage characteristics of β-Ga_2O_3 trench Schottky barrier diodes. Appl Phys Lett, 2020, 116, 152104

[93] Wilhelmi F, Kunori S, Sasaki K, et al. Packaged β-Ga_2O_3 trench MOS Schottky diode with nearly ideal junction properties. IEEE Trans Power Electron, 2022, 37, 3737

[94] Neal A T, Mou S, Lopez R, et al. Incomplete ionization of a 110 meV unintentional donor in β-Ga_2O_3 and its effect on power devices. Sci Rep, 2017, 7, 13218

[95] Zhou F, Gong H H, Xiao M, et al. An avalanche-and-surge robust ultrawide-bandgap heterojunction for power electronics. Nat Commun, 2023, 14, 4459

[96] Wang C L, Gong H H, Lei W N, et al. Demonstration of the p-NiO_x/n-Ga_2O_3 heterojunction gate FETs and diodes with $BV^2/R_{on,sp}$ figures of merit of 0.39 GW/cm^2 and 1.38 GW/cm^2. IEEE Electron Device Lett, 2021, 42, 485

[97] Zhou F, Gong H H, Wang Z P, et al. Over 1.8 GW/cm^2 beveled-mesa NiO/β-Ga_2O_3 heterojunction diode with 800 V/10 A nanosecond switching capability. Appl Phys Lett, 2021, 119, 262103

[98] Hao W B, He Q M, Zhou X Z, et al. 2.6 kV NiO/Ga_2O_3 heterojunction diode with superior high-temperature voltage blocking capability. 2022 IEEE 34th International Symposium on Power Semiconductor Devices and ICs (ISPSD), 2022, 105

[99] Zhang J C, Dong P F, Dang K, et al. Ultra-wide bandgap semiconductor Ga_2O_3 power diodes. Nat Commun, 2022, 13, 3900

[100] Xiao M, Wang B Y, Spencer J, et al. NiO junction termination extension for high-voltage (>3 kV) Ga_2O_3 devices. Appl Phys Lett, 2023, 122, 183501

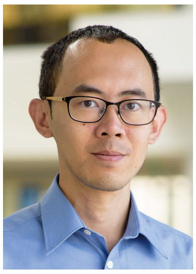

Man Hoi Wong is an Associate Professor at the Department of Electronic and Computer Engineering at the Hong Kong University of Science and Technology (HKUST). He received his Ph.D. from the University of California Santa Barbara, USA, in 2009. Prof. Wong has worked at the SEMATECH corporate research consortium in the USA and the National Institute of Information and Communications Technology in Japan as a research scientist. Prior to joining HKUST, he was an Assistant Professor at the University of Massachusetts Lowell, USA. His current research focuses on ultrawide-bandgap semiconductor materials and power devices.